

Engineered Low Temperature Hydrothermal Synthesis of Phase-Pure Lead-Based Perovskites Using Ethylenediamine Tetra-acetic Acid Complexation

Bonnie Gersten,^{*,†,‡} Małgorzata Lencka,[§] and Richard Riman[†]

Department of Ceramics, College of Engineering, Rutgers, The State University of New Jersey, Piscataway, New Jersey 08854-8065, OLI Systems, Inc., 108 American Road, Morris Plains, New Jersey 07950

Received May 15, 2000. Revised Manuscript Received June 1, 2001

Thermodynamic modeling of hydrothermal solutions was used to examine the influence of ethylenediamine tetra-acetic acid (EDTA) on the synthesis of lead-based perovskites, PbTiO_3 and $\text{PbZr}_{0.52}\text{Ti}_{0.48}\text{O}_3$. Temperature, pH, input reagent concentrations, and $\text{Pb}/(\text{Ti} + (\text{Zr}))$ and Pb/EDTA ratios were examined. Thermodynamic calculations from 25 to 100 °C indicated that, when the Pb/EDTA and $\text{Pb}/(\text{Ti} + (\text{Zr}))$ molar ratios were 2.0 and Pb input concentration was 0.1 M, phase-pure perovskites formed across the greatest pH range (7–14+). Precipitation of unwanted unary lead phases such as PbO was suppressed in all cases. In the absence of EDTA and solutions containing a molar excess of lead ions, the formation of phase-pure perovskites was limited to narrow pH ranges (5–8 and above 14) because of PbO precipitation. Theoretical predictions were experimentally validated with use of X-ray diffraction, transmission electron microscopy, energy dispersive spectrometry, and atomic absorption spectroscopy. Experimental results validated the theoretical predictions at temperatures above a minimum reaction temperature. Relative to comparable hydrothermal systems free of EDTA, the addition of EDTA was found to lower the minimum reaction temperature by 70 °C for PbTiO_3 (70 °C) and 25 °C for $\text{PbZr}_{0.52}\text{Ti}_{0.48}\text{O}_3$ (125 °C).

Introduction

Hydrothermal synthesis has been used for the preparation of multicomponent anhydrous crystalline ceramic oxide powders for processing a variety of electroceramic materials with enhanced properties.¹ Hydrothermal synthesis offers the capability to control particle size, aggregation, and morphology but maintains a high degree of purity and uniformity. Furthermore, the process can be designed to be environmentally benign, use inexpensive reactants, and consume less energy than conventional powder synthesis processes because of low reaction temperatures. However, to obtain phase-pure materials, optimal process conditions (i.e., pH, temperature, and initial reagent concentrations) need to be identified. The number of experiments required to find these conditions can be significantly reduced by calculating yield diagrams of perovskites using thermodynamic modeling, as has been demonstrated for electroceramic ABO_3 perovskites such as PbTiO_3 ,^{2,3} BaTiO_3 ,^{3–5} SrTiO_3 ,⁴ CaTiO_3 ,⁴ $\text{Pb}(\text{Zr},\text{Ti})\text{O}_3$,⁶ and SrZrO_3 .⁷

Low reaction temperatures (<100 °C) would also be ideal to facilitate reactions that can proceed at atmospheric pressure, which will allow the use of inexpensive Teflon-lined reflux condenser-based reactor technology. In addition, such technology will eliminate the safety hazards associated with pressure vessels. To this end, this article focuses on finding precursor-based pathways for low hydrothermal reaction temperatures for PbTiO_3 and $\text{Pb}(\text{Zr}_{0.52}\text{Ti}_{0.48})\text{O}_3$.

To find conditions that facilitate rapid low-temperature formation of hydrothermal lead-based perovskites, classical kinetics variables such as the concentration of soluble lead ions can be increased to higher levels. However, previous work has shown that the precipitation of lead components occurs during precursor preparation and/or the use of a stoichiometric excess of lead over that of the B-site ion [e.g., $\text{Pb}/(\text{Ti} + \text{Zr}) > 1$]. The precipitation of phases such as unary lead oxide limits the rate of release of soluble lead for driving the equilibria for PbTiO_3 formation. In lead-excess systems, lead-containing impurity phases remain, which must be washed from the perovskite powder by using acetic acid solutions.^{8–14} However, this approach may also leach lead species from the perovskite phase, as shown by

* To whom correspondence should be addressed.
† Rutgers, The State University of New Jersey.

‡ Current address: Army Research Laboratory, AMSRL-WM-MD, Aberdeen Proving Ground, MD 21005-5069.

§ OLI Systems, Inc.

- (1) Dawson, W. *Ceram. Bull.* **1988**, *67*, 1673.
- (2) Lencka, M. M.; Riman, R. E. *J. Am. Ceram. Soc.* **1993**, *76*, 2649.
- (3) Lencka, M. M.; Riman, R. E. *Chem. Mater.* **1993**, *5*, 61.
- (4) Lencka, M. M.; Riman, R. E. *Chem. Mater.* **1995**, *7*, 18.
- (5) Bendale, P.; Venigalla, S.; Ambrose, J. R.; Vernick, E. D., Jr.; Adair, J. H. *J. Am. Ceram. Soc.* **1993**, *76*, 2619.
- (6) Lencka, M. M.; Anderko, A.; Riman, R. E. *J. Am. Ceram. Soc.* **1995**, *78*, 2609.

(7) Lencka, M. M.; Nielson, E.; Riman, R. E. *Chem. Mater.* **1997**, *9*, 1116.

(8) Ohaba, Y.; Rikitoku, T.; Tsurumi, T.; Daimon, M. *J. Ceram. Soc. Jpn.* **1996**, *104*, 6.

(9) Li, Y. X.; Yao, X. *Sens. Actuators, A* **1993**, *35*, 255.

(10) Sato, S.; Murakata, T.; Yanagi, H.; Miyasaka, F.; Iwaya, S. *J. Mater. Sci.* **1994**, *29*, 5657.

(11) Kaneko, S.; Imoto, F. *Bull. Chem. Soc. Jpn.* **1978**, *51*, 1739.

calculated stability diagrams.² These problems could be avoided if precipitation of unary lead-bearing species could be avoided altogether. The use of complexing agents such as ethylenediaminetetraacetic acid (EDTA, $C_{10}H_{16}N_2O_8$) offers such an opportunity.

In previous work, EDTA and other chelating complexes were used for the homogeneous precipitation of amorphous powders at temperatures of 25–90 °C, which could be calcined at temperatures greater than 500 °C to crystallize $CaTiO_3$,¹⁵ $Pb_3Nb_2O_8$,^{15,16} and $BaTiO_3$.¹⁷ However, $PbTiO_3$ ¹⁸ could not be prepared with EDTA even with a calcination step. With thermodynamic computations guiding the design and execution of experiments, it should be possible to design EDTA-based precursor systems that lead to the direct precipitation of $PbTiO_3$ or other lead-based perovskites. EDTA prevents the formation of lead oxide so that the process is no longer dissolution rate-limited by the lead component and thus should proceed in a more labile fashion. In addition, the ability to use a stoichiometric excess of lead should further enhance the reaction kinetics by increasing the soluble lead concentration. Finally, the use of thermodynamic modeling will also enable finding reaction conditions that facilitate a broad range of concentration and pH across which lead-based perovskites are stable.

The objective of this article is to use thermodynamic modeling to find low-temperature hydrothermal reaction conditions using EDTA that eliminate phase heterogeneities (e.g., PbO and TiO_2), yet provide a broad pH range for making $PbTiO_3$ and $Pb(Zr,Ti)O_3$. Our overall approach is to develop a thermodynamic model, compute stability and yield diagrams, validate the equilibrium models, and identify the minimum reaction temperatures for formation of each perovskite phase.

Thermodynamic Model

The thermodynamic model for simulating the hydrothermal synthesis of $PbTiO_3$ ^{2,3} and $Pb(Zr,Ti)O_3$ ⁶ in a multicomponent aqueous system has been described previously for solutions that do not contain EDTA. The application of the model requires the knowledge of the standard Gibbs energies ΔG_f° and enthalpies ΔH_f° of formation, entropies S° at a reference temperature (298.15 K), as well as partial molar volumes V° and heat capacities C_p° as functions of temperature for all species (aqueous and solid) in solution. Calculations were made assuming lead acetate ($PbAc_2$), titania (TiO_2 , anatase phase), EDTA, zirconia (ZrO_2), and potassium hydroxide (KOH) comprised the precursor system. The standard-state properties for all known aqueous and solid species in the Pb – Ti – (Zr) – K –(EDTA)– H_2O system were obtained from experimental values or were estimated.¹⁹ Table 1 lists additional relevant equilibria for the Pb –

Table 1. Additional Relevant Reaction Equilibria in the Pb – Zr – Ti –EDTA Hydrothermal System

1. $(C_{10}H_{14}N_2O_8)^{2-} = H^+ + (C_{10}H_{13}N_2O_8)^{3-}$
2. $(C_{10}H_{15}N_2O_8)^{1-} = H^+ + (C_{10}H_{14}N_2O_8)^{2-}$
3. $(C_{10}H_{17}N_2O_8)^{1+} = H^+ + C_{10}H_{16}N_2O_8(aq)$
4. $C_{10}H_{16}N_2O_8(s) = C_{10}H_{16}N_2O_8(aq)$
5. $C_{10}H_{16}N_2O_8(vap) = C_{10}H_{16}N_2O_8(aq)$
6. $(C_{10}H_{18}N_2O_8)^{2+} = H^+ + (C_{10}H_{17}N_2O_8)^{1+}$
7. $(C_{10}H_{13}N_2O_8)^{3-} = H^+ + (C_{10}H_{12}N_2O_8)^{4-}$
8. $K(C_{10}H_{12}N_2O_8)^{3-} = K^+ + (C_{10}H_{13}N_2O_8)^{2-}$
9. $Pb(C_{10}H_{12}N_2O_8)^{2-} = Pb^{2+} + (C_{10}H_{13}N_2O_8)^{3-}$
10. $Pb(HC_{10}H_{12}N_2O_8)^{1-} = H^+ + Pb(C_{10}H_{12}N_2O_8)^{2-}$
11. $Zr(C_{10}H_{12}N_2O_8) = Zr^{4+} + (C_{10}H_{12}N_2O_8)^{4-}$
12. $Ti(C_{10}H_{12}N_2O_8) = Ti^{4+} + (C_{10}H_{12}N_2O_8)^{4-}$
13. $Na(C_{10}H_{12}N_2O_8)^{3-} = Na^+ + (C_{10}H_{13}N_2O_8)^{2-}$

Ti – (Zr) – K –(EDTA)– H_2O system not provided in previous papers.^{2,6}

The standard-state thermochemical properties (i.e., ΔG_f° , ΔH_f° , and S°) for EDTA and its nonmetallic complexes (cf. Table 1, eqs 1–7) were calculated on the basis of apparent equilibrium constants for the species above reported by Martell and Smith^{20–22} and thermodynamic (i.e., at infinite dilution) equilibrium constants given by Yalkowski.²³ Equilibrium constants for EDTA and its complexes were given in the temperature range from 0 to 100 °C by Yalkowski²³ and from 20 to 25 °C by Martell and Smith.^{20–22} Standard-state heat capacities were taken from Hovey and Tremaine.²⁴ Parameters for the Helgeson–Kirkham–Flowers equation were calculated by the method of Anderson et al.²⁵ Because equilibrium constants for EDTA and its complexes were developed for temperatures less than 100 °C, calculations at higher temperatures should be made with caution.

Standard-state properties for Pb, Zr, Ti, K, and Na complexes of EDTA (cf. Table 1, eqs 8–13) were calculated from the apparent equilibrium constants and/or enthalpy and entropy of reactions data taken from the compilations of Martell and Smith.^{20–22} The apparent equilibrium constants are usually reported at 20 and 25 °C at ionic strengths from 0.01 to 0.1 m. They were recalculated into thermodynamic equilibrium constants and subsequently into standard-state Gibbs free energy, enthalpy, and entropy. Again, calculations at higher temperatures may be subject to considerable uncertainty because the primary experimental data were limited to ambient conditions. Activity coefficients were calculated for all species in the hydrothermal system. In many cases, the activity coefficient model parameters were obtained by regressing experimental thermodynamic data (e.g., vapor pressure, solid solubilities). If primary experimental data were not available, as was the case for most EDTA aqueous species, the model substance approach was used.²⁶ According to the model substance approach, the activity coefficients for 1:1 cation–anion pairs were assumed to be equivalent to

(12) Kutty, T. R. N.; Balachandran, R. *Mater. Res. Bull.* **1984**, *19*, 1479.
 (13) Beal, K. C. *Ceramic Powder Science*; The American Ceramic Society: Westerville, OH, 1987; Vol. 21, p 33.
 (14) Ichihara, T.; Tsurumi, T.; Asaga, K.; Lee, K. H.; Daimon, M. *J. Ceram. Soc. Jpn. Int. Ed.* **1990**, *98*, 155.
 (15) Kim, M. J.; Matijevic, E. *J. Am. Ceram. Soc.* **1994**, *77*, 1950.
 (16) Kim, M. J.; Matijevic, E. *J. Mater. Res.* **1991**, *6*, 840.
 (17) Gherardi, P.; Matijevic, E. *Colloids Surf.* **1988**, *32*, 257.
 (18) Kim, M. J.; Matijevic, E. *Chem. Mater.* **1989**, *1*, 363.
 (19) *Environmental and Corrosion Simulation Program (ESP/CSP)*, version 6.0; OLI Systems, Inc.: Morris Plains, NJ, 1998.

(20) Martell, A. E.; Smith, R. M. *Critical Stability Constants*; Amino Acids, Vol. 1; Plenum Press: New York, 1974.
 (21) Martell, A. E.; Smith, R. M. *Critical Stability Constants*; First Supplement, Vol. 5; Plenum Press: New York, 1982.
 (22) Martell, A. E.; Smith, R. M. *Critical Stability Constants*; Second Supplement, Vol. 6; Plenum Press: New York, 1989.
 (23) Yalkowski, S. H. *Pharmaceutical Sciences*, College of Pharmacy, University of Arizona, Tucson. Private communication, 1993.
 (24) Hovey, J. K.; Tremaine, P. R. *J. Phys. Chem.* **1985**, *89*, 5541.
 (25) Anderson, G. M.; Castet, S.; Schott, J.; Mesmer, R. E. *Geochim. Cosmochim. Acta* **1991**, *55*, 1769.
 (26) Venezky, D. L.; Moniz, W. B. *Anal. Chem.* **1969**, *41*, 11.

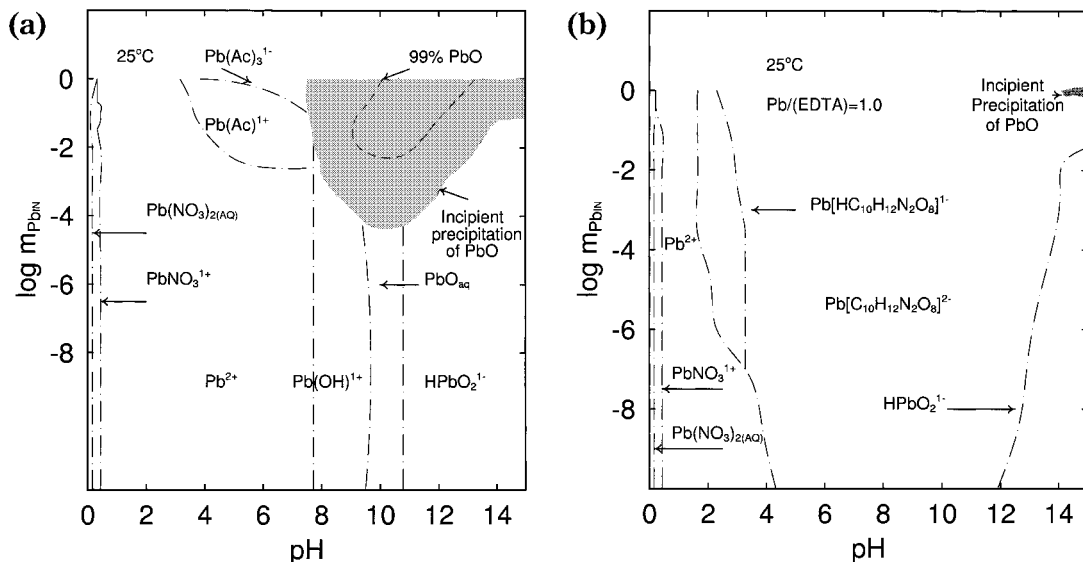


Figure 1. Yield diagrams for lead species as a function of pH. (a) $\text{Pb-K-H}_2\text{O}$ and (b) $\text{Pb-K-EDTA-H}_2\text{O}$.

those for the $\text{Na}^+ \text{Cl}^-$ pair; those for 1:2 cation–anion pairs were assumed to be equivalent to those for the $\text{Na}^+ \text{CO}_3^{2-}$ pair; those for 2:1 cation–anion pairs were assumed to be equivalent to those for the $\text{Ca}^{2+} \text{Cl}^-$ pair; and those for 2:2 cation–anion pairs were assumed to be equivalent to those for the $\text{Zn}^{2+} \text{SO}_4^{2-}$ pair. For interactions that involve species with -3 and -4 charges, the values were assumed the same as for those with the -2 charge. In some cases, as in the EDTA ions, structural similarity was also important in choosing a model substance. For nitrilotriacetic acid complex systems discussed later in this article, a private data bank¹⁹ was used; it will not be reported here for purposes of brevity and the preliminary nature of the computations.

The thermodynamic model was used to construct diagrams of total input lead concentration (m_{PbIN}) versus equilibrium pH, which show the stability and yield of the aqueous species and solid products for the following systems with and without the use of EDTA. These are namely (1) $\text{Pb-K-(EDTA)-H}_2\text{O}$ (Figure 1a, b) (2) $\text{Pb-Ti-K-(EDTA)-H}_2\text{O}$ (Figure 2a–f), (3) $\text{Pb-Ti-Zr-K-(EDTA)-H}_2\text{O}$ (Figure 3a–f). Stability and yield diagrams for equilibrium pH or KOH molality as a function of temperature were plotted for $\text{Pb-Ti-K-(EDTA)-H}_2\text{O}$ (Figure 4a–h), and $\text{Pb-Ti-Zr-K-(EDTA)-H}_2\text{O}$ (Figure 5a, b) systems. The dominant aqueous species and boundaries between various dominant aqueous species fields were included in the $\text{Pb-K-(EDTA)-H}_2\text{O}$ systems but are not shown in the other diagrams for simplicity. Four kinds of boundaries are represented in the diagrams. The first boundary line is between two aqueous species that corresponds to the loci where the two species have equal concentrations. A second is the boundary line between solid and aqueous species, which corresponds to complete disappearance of solid phase (solubility curve). In practice, this corresponds to less than 0.25 mol % (hereon in, referred to as %) of the reactant found in the solid phase. The third is a boundary that represents the beginning of the 99% yield region for perovskite PbTiO_3 or $\text{PbZr}_{0.52}\text{Ti}_{0.48}\text{O}_3$ or solid PbO . The fourth boundary lies between two solid phases located within the stability region of the perovskite. It denotes the incipient precipitation of a second phase (e.g., PbO). Calculations were performed at 25, 70, 125,

145, and 200 °C to show temperature-induced changes in equilibria and to facilitate comparison between various chemical precursor systems.

Yield diagrams (Figures 1–3) are displayed with uniform notation for consistency. Dot-dashed lines (Figure 1a, b) represent boundaries between aqueous species. Dark shaded regions (Figures 1a, b, 2a, and 3a) represent the stability region of PbO . The area above a dashed line within a dark shaded region (Figure 1a) denotes greater than 99% precipitation of PbO . For the perovskite systems (Figures 2a–d and 3a–d), the solid lines show the incipient precipitation of perovskite for $\text{Pb}/(\text{Ti} + (\text{Zr}))$ ratios equal to 1.0 and/or 2.0. Outside these lines (toward lower pH) unreacted reagents in the form of aqueous Pb , Ti , (Zr) , EDTA, and solid TiO_2 (and ZrO_2) are present. The light-gray shaded region denotes the greater than 99% perovskite yield for the $\text{Pb}/(\text{Ti} + (\text{Zr}))$ ratio equal to 2.0 (Figures 2a, c, d and 3a, c, d). In contrast, for the $\text{Pb}/(\text{Ti} + (\text{Zr}))$ ratio equal to 1.0, the dashed line within the shaded region denotes the greater than 99% perovskite yield (Figures 2b–d and 3b–d). Between the solid lines and the light-gray area or dashed-line light-gray area, unreacted reagents and perovskite are present in proportions ranging from 0 to 99%.

Yield diagrams were also constructed for equilibrium pH versus temperature for $\text{Pb-Ti-K-(EDTA)-H}_2\text{O}$ (Figure 4a, c, e, g) and $\text{Pb-Ti-Zr-K-(EDTA)-H}_2\text{O}$ (Figure 5a) systems at m_{PbIN} equal to 0.1 mol/kg H_2O . Diagrams were also plotted for input KOH molality as a function of temperature for $\text{Pb-Ti-K-(EDTA)-H}_2\text{O}$ (Figure 4b, d, f, h) and $\text{Pb-Ti-Zr-K-(EDTA)-H}_2\text{O}$ (Figure 5b) systems to fully specify the input reaction conditions. The area set by the pH or KOH molality equal to zero and the dashed line represents the region where perovskite precipitation does not occur. Only secondary phases (e.g., titania, zirconia, EDTA, and all aqueous species in solution) are present in this region. The dashed line represents the beginning of perovskite precipitation. The region between the dashed and solid line comprises a mixture of perovskite (0–99%) and secondary phases. The region above the solid line signifies greater than 99% yield of perovskite.

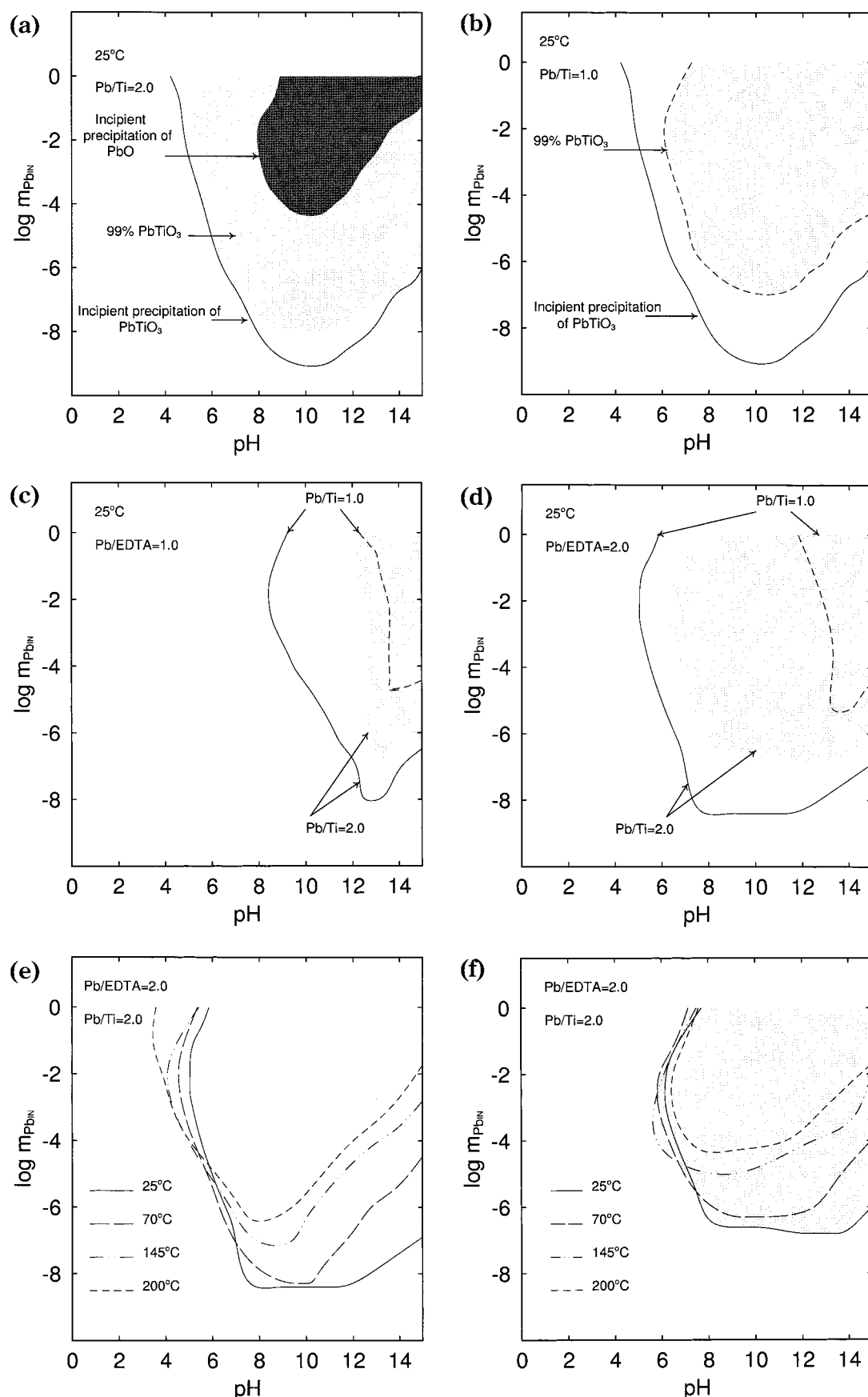


Figure 2. The yield diagram for the $\text{Pb}-\text{Ti}-\text{K}-(\text{EDTA})-\text{H}_2\text{O}$ system for input lead species molality as a function of pH with (a) $\text{Pb}/\text{Ti} = 2.0$ and (b) $\text{Pb}/\text{Ti} = 1.0$; the yield diagrams for the $\text{Pb}-\text{Ti}-\text{EDTA}-\text{H}_2\text{O}$ system with (c) $\text{Pb}/\text{EDTA} = 1.0$ and (d) $\text{Pb}/\text{EDTA} = 2.0$. The (e) stability and (f) 99% yield diagrams for the $\text{Pb}-\text{Ti}-\text{EDTA}-\text{H}_2\text{O}$ system with $\text{Pb}/\text{EDTA} = 2.0$ and $\text{Pb}/\text{Ti} = 2.0$ for temperatures 25–200 °C.

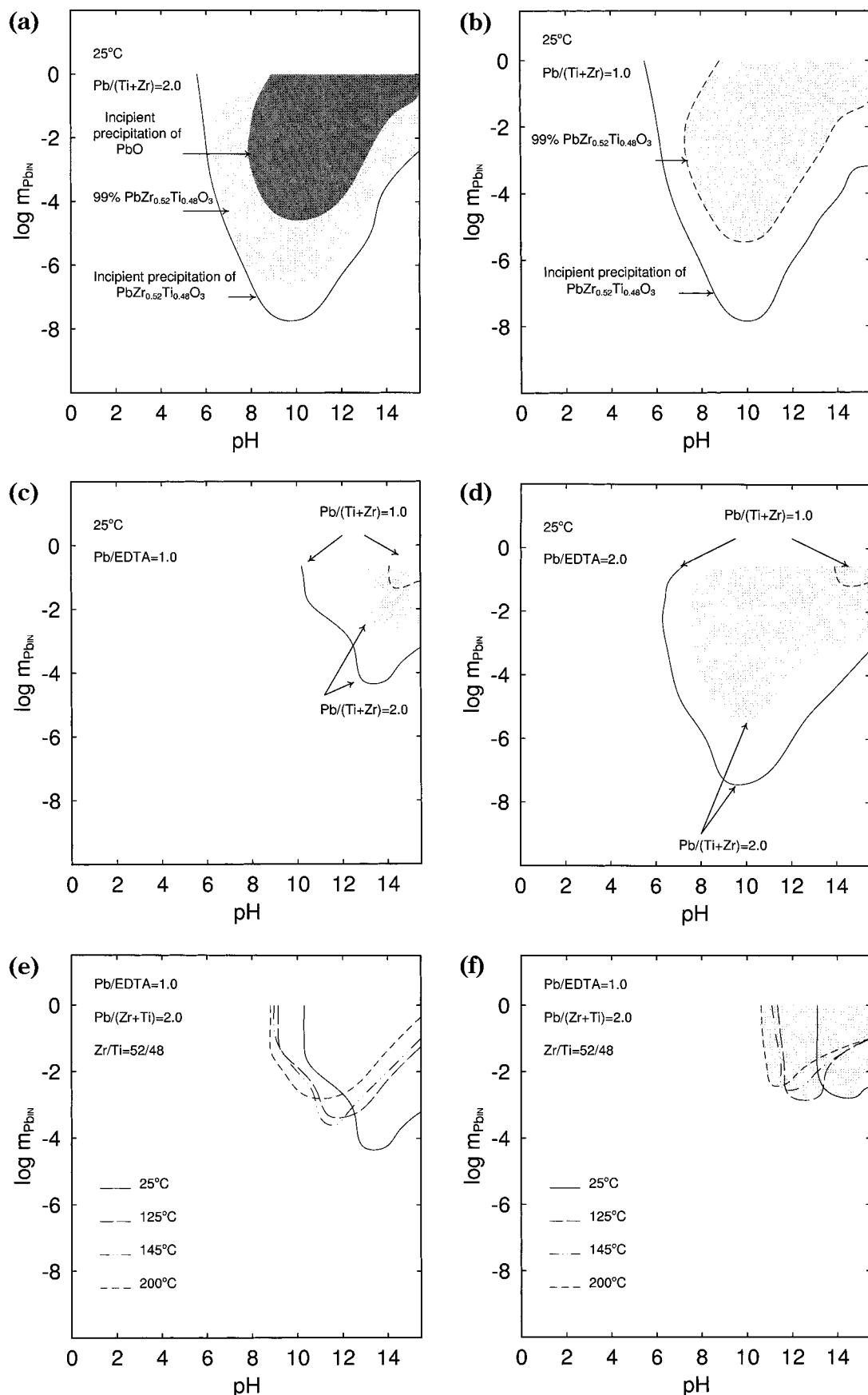


Figure 3. The yield diagram for the $\text{Pb-Zr-Ti-K-(EDTA)-H}_2\text{O}$ system with (a) $\text{Pb}/(\text{Ti}+\text{Zr})=2.0$ and (b) $\text{Pb}/(\text{Ti}+\text{Zr})=1.0$ and the yield diagram for the $\text{Pb-Zr-Ti-EDTA-H}_2\text{O}$ system for input lead species molality as a function of pH with (c) $\text{Pb}/\text{EDTA}=1.0$ and (d) $\text{Pb}/\text{EDTA}=2.0$. The (e) stability and (f) 99% yield diagrams for the $\text{Pb-Zr-Ti-EDTA-H}_2\text{O}$ system with $\text{Pb}/\text{EDTA}=1.0$ and $(\text{Pb}/(\text{Ti}+\text{Zr})=2.0$ for temperatures $25-200^\circ\text{C}$.

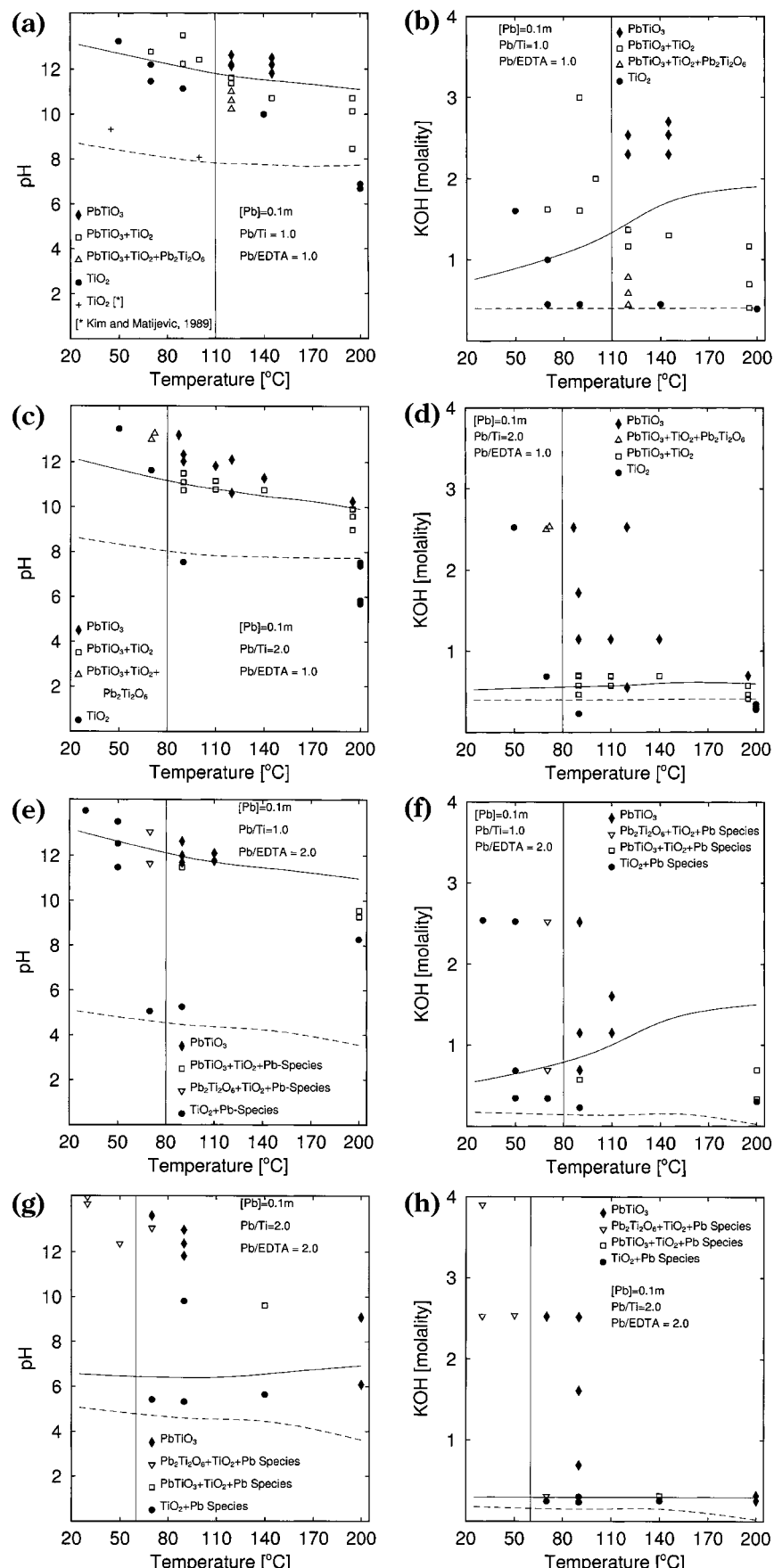


Figure 4. Yield diagrams for the $\text{Pb}-\text{Ti}-\text{K}-\text{EDTA}-\text{H}_2\text{O}$ system pH or KOH molarity as a function of temperature. Diagrams for $\text{Pb}/\text{EDTA}=1$ and $\text{Pb}/\text{Ti}=1$ with (a) pH and (b) KOH as dependent variables. Diagrams with $\text{Pb}/\text{EDTA}=1$ and $\text{Pb}/\text{Ti}=2$ are plotted with (c) pH and (d) KOH molarity as dependent variables. Diagrams for $\text{Pb}/\text{EDTA}=2$ and $\text{Pb}/\text{Ti}=1$ are plotted with (e) pH and (f) KOH molarity as dependent variables. Diagrams for $\text{Pb}/\text{EDTA}=2$ and $\text{Pb}/\text{Ti}=2$ are plotted with (g) pH and (h) KOH as dependent variables.

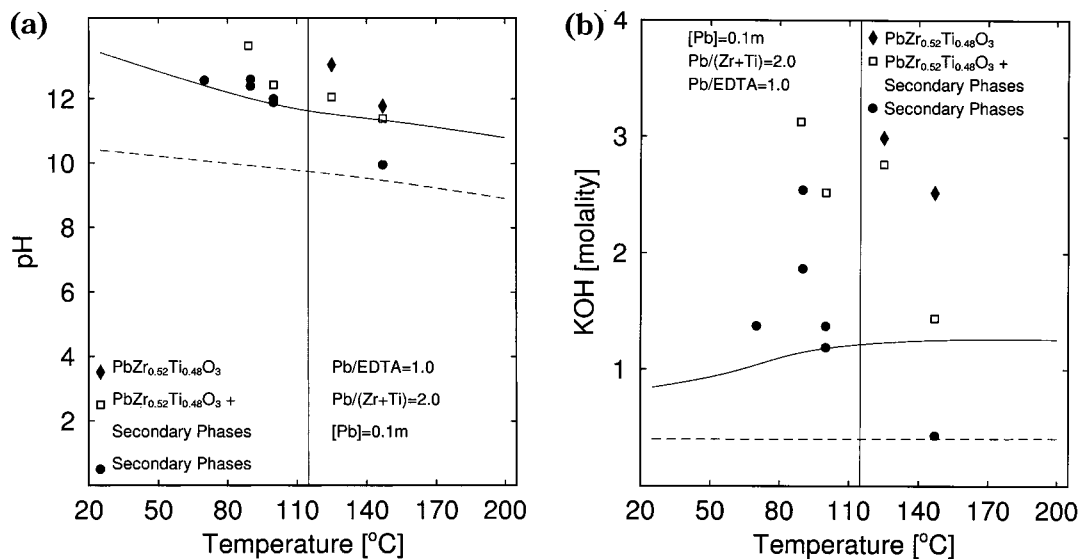


Figure 5. Yield diagrams for the Pb-Ti-Zr-K-EDTA-H₂O. (a) PbZr_{0.52}Ti_{0.48}O₃ with Pb/EDTA = 1.0 and Pb/(Ti + Zr) = 2.0 for pH as a function of temperature. (b) PbZr_{0.52}Ti_{0.48}O₃ with Pb/EDTA = 1.0 and Pb/(Ti + Zr) = 1.0 for KOH molality as a function of temperature.

Figure 1a, b shows the stability and yield diagrams for the Pb-(EDTA)-H₂O system without and with EDTA, respectively. Figure 1a shows the loci for lead hydroxyl complexes and the stability region (shaded) for solid PbO. The area encompassed by the dashed line represents the greater than 99% yield of solid PbO phase. The chemical identity of aqueous lead species denoted by the dot-dashed lines varies with pH and lead molality. The amphoteric nature of lead accounts for the parabolic shape of the PbO stability region. From Figure 1a, PbO precipitation occurs between pH values of 8 and 14+ when m_{PbIN} is equal to 0.1 mol/kg H₂O at 25 °C. Thus, at room temperature, the typical pH values and lead concentrations used for hydrothermal experimentation will form PbO precipitate. This is because the titanium and zirconium precursors are too unreactive at this temperature⁶ to consume the free lead to form a perovskite reaction product and therefore do not compete for lead at this temperature. Because both lead titanate and lead zirconate titanate form in the pH range where PbO can precipitate,^{2,6} reaction conditions must be found that suppress lead oxide formation yet provide soluble lead for perovskite precipitation.

Figure 1b shows the influence of EDTA on PbO_(s) stability when the Pb/EDTA molar ratio is equal to 1.0. In this case, lead remains in solution at m_{PbIN} values less than 0.8 mol/kg H₂O for almost all pH values. However, PbO precipitation occurs between a pH value of 13 and higher at 25 °C, which does not overlap significantly with the stability regions for either lead titanate or lead zirconate titanate. These initial findings suggest that EDTA will suppress formation of lead oxide in solution. However, the key question is whether it also suppresses formation of either of the lead perovskites.

Figure 2a-d shows the stability and yield calculations of the solid products in the Pb-Ti-(EDTA)-H₂O system. Figure 2a, b shows the stability and yield diagrams without EDTA for the Pb/Ti ratios equal to 2.0 and 1.0, respectively. The stability and yield regions of perovskite are parabolic, similar in shape as described for PbO precipitation (Figure 1a). Similar results are shown in previous reports² for higher temperatures, 80 and 160

°C, but have been reported here at 25 °C. Temperature does not significantly change the perovskite precipitation region at practical m_{PbIN} concentrations (i.e., above 10⁻¹ mol/kg H₂O). Comparing diagrams with and without a molar excess highlights the effect of a molar excess of lead with respect to titanium on PbTiO₃ precipitation when EDTA is not present. With a molar excess, when the Pb/Ti molar ratio is equal to 2.0 (Figure 2a), PbO precipitation occurs along with PbTiO₃. The maximum pH range on the diagram (pH window) for pure PbTiO₃ formation is 5–8.5 and greater than 14 (Figure 2a). When the Pb/Ti molar ratio is 1.0, the pH window extends from 6.5 to 14+ (Figure 2b). However, as mentioned earlier, despite this wide pH range, precipitation of unary lead phases during precursor preparation make this system undesirable.

Figure 2c shows the yield diagram of PbTiO₃ with a Pb/EDTA ratio equal to 1.0 and for Pb/Ti ratios equal to either 1.0 or 2.0. Lead titanate stability fields can be seen in all diagrams. Thus, it can be concluded that lead EDTA complexation does not completely suppress lead titanate formation. By increasing the Pb/Ti ratio from 1.0 to 2.0, the pH window for precipitation of PbTiO₃ is enlarged by 1 pH unit (Figure 2c). Use of a Pb/Ti ratio equal to 2.0 does not lead to precipitation of an undesirable phase such as PbO (Figure 2a). This is due to the complexing action of EDTA with lead species that are in excess with respect to the titanium species. However, when EDTA is present, the region for phase-pure perovskite is also shifted to higher pH (pH values greater than 12), which provides a much smaller operating window for phase-pure perovskite than when EDTA is not present (pH equal to 5–8 and greater than 14, Figure 2a). These results show that to some degree EDTA complexation plays a role in suppressing perovskite formation, owing to its high thermodynamic stability.

Figure 2d shows the yield diagram of PbTiO₃ with a Pb/EDTA ratio equal to 2.0 and for Pb/Ti ratios equal to either 1.0 or 2.0. With use of a Pb/EDTA ratio of 2.0 and a Pb/Ti ratio of 1.0, a yield field approximately 2 pH units wide results, which is comparable to what is

Table 2. Summary of Calculated and Experimental Hydrothermal Reaction Conditions for Phase Pure PT and PZT

sample	system	Pb/(Ti + (Zr))	Pb/EDTA	experimental T_{\min} (°C)	calculated pH span at 25 °C ^a	experimental pH range	experimental KOH _{min} (m) ^b	figure(s)
1	PT	2.0	no	140 ^c	5–8.0 and > 14	6 ^{c,d}		2a
2	PT	1.0	no	140 ^c	6.0 to > 14	7 to 10 ^c		2b
3	PT	2.0	1.0	90	11.5 to > 14	10 to > 14	0.6	2c, 4c, 4d
4	PT	1.0	1.0	120	12.2 to > 14	12 to > 14	2.5	2c, 4a, 4b
5	PT	2.0	2.0	70	6.0 to > 14	6 to > 14	0.6	2d, 2e, 2f, 4g, 4h
6	PT	1.0	2.0	90	> 14	12 to > 14	0.6	2d, 4e, 4f
7	PZT	2.0	no		6.5–8 and > 14			3a
8	PZT	1.0	no	150 ^e	8 to 14	9 to 12 ^e		3b
9	PZT	2.0	1.0	125	13 to > 14	12 to > 14	2.5	3c, 3e, 3f, 5a, 5b
10	PZT	1.0	1.0		> 14			3c
11	PZT	2.0	2.0		8 to > 14			3d
12	PZT	1.0	2.0		> 14			3d

^a The pH window was determined at 25 °C because this is a convenient temperature for pH measurement. ^b Minimum molality of KOH necessary for precipitation of phase-pure lead-based perovskite. ^c ref 2. ^d Pb/Ti is 1.5 instead of 2.0. ^e ref 6.

achieved with a Pb/EDTA ratio of 1.0 and a Pb/Ti ratio of 2.0. However, when the Pb/Ti ratio and Pb/EDTA ratio are both increased to 2.0, the pH span widens considerably 8 pH units. In both cases, again, PbO precipitation is not observed. This broadening of the stability region, caused by the higher Pb/EDTA ratio for both Pb/Ti ratios, can be attributed to the large amount of uncomplexed lead ions, which are available for lead titanate formation but not high enough in concentration to precipitate the PbO phase. The appreciable concentration of uncomplexed lead for the EDTA-based system makes the pH span of its yield field (Figure 2d) very similar to a system having a Pb/Ti ratio equal to 1.0 without EDTA (Figure 2b). The presence of uncomplexed lead species also suggests that systems containing Pb/EDTA ratios of 2.0 may also be prone to formation of unary lead phases during precursor preparation, as discussed earlier for non-EDTA-containing lead-based systems such as Pb–K–H₂O or Pb–Ti–K–H₂O. The relevance of this issue is deliberated later.

Figure 2e shows the stability yield diagrams for the PbTiO₃ for the Pb/Ti and Pb/EDTA ratios equal to 2.0 at temperatures of 25, 70, 145, and 200 °C. The various boundaries represent the incipient precipitation boundaries of PbTiO₃ corresponding to temperatures shown in the legend. As shown in Figure 2e, as temperature increases, the incipient precipitation boundary shifts toward lower pH. The lower pH boundary for 99% yield fields for PbTiO₃ (Figure 2f) changes with temperature depending on m_{PbIN} . For instance, at 0.1 m_{PbIN} as temperature increases, the 99% yield boundary pH increases while the incipient precipitation boundary pH decreases (Figure 4g). At all other m_{PbIN} values, the position of the 99% yield boundary does not vary with temperature in a systematic fashion.

The yield diagrams shown in Figure 4 emphasize two important points. First, the dependence of KOH concentration on temperature for the 99% yield boundary is very sensitive to a range of precursor concentration variables. For instance, when the Pb/Ti ratio is 2.0, the KOH concentration required for 99% yield is independent of temperature (Figure 4d). In contrast, when the Pb/Ti is equal to 1.0, the KOH concentration is dependent on temperature (Figure 4b). Second, small changes in KOH concentration can transition the reaction from partially complete to 99%+ yields. For example, at 25 °C, the difference between the incipient precipitation boundary and the 99% yield boundary for Figure 4d is 0.13 M KOH units, but this difference corresponds to

~3.5 pH units, which represents 3.5 orders of magnitude difference in the hydronium ion concentration. At 160 °C, this difference reduces to 2.5 orders of magnitude.

The thermodynamic model was also used to compute diagrams to determine the stability and yield of PbZr_{0.52}–Ti_{0.48}O₃ in the Pb–Ti–Zr–(EDTA)–H₂O system. Figures 3 and 5 and Table 2 summarize these findings. The equilibrium behavior of this system is similar to what was found for PbTiO₃. First, EDTA suppresses PbO formation to facilitate the use of hydrothermal solutions containing an excess of lead [i.e., Pb/(Zr+Ti) = 2.0] rather than being limited to only stoichiometric solutions [i.e., Pb/(Zr+Ti) = 1.0], which is necessary for systems free of EDTA (Figure 3a–d). Second, as with PbTiO₃, an excess of lead broadens the pH window by about 1 pH unit. When Pb/(Zr + Ti) equals 2.0, increasing the Pb/EDTA ratio from 1.0 to 2.0 broadens the pH window by about 5 pH units (Figure 3c, d). Temperature serves to reduce the pH required for incipient precipitation and 99% yield under optimum conditions where both Pb/EDTA and Pb/(Zr + Ti) ratios are equal to 1.0 and 2.0, respectively (Figure 3e, f). Although counter intuitive, input concentrations of KOH increase with a corresponding decrease in equilibrium pH (Figure 5a, b).

Experimental Section

Synthesis. Lead acetate trihydrate (Aldrich, Milwaukee, WI; Fisher Scientific, Fair Lawn, NJ; purity 99%), potassium hydroxide (Fisher Scientific, purity >85%, ~15% water, below 0.4% K₂CO₃) and EDTA (Fisher Scientific, purity 99.6%) were used as a lead source, pH adjuster, and chelating agent, respectively. Titanium dioxide (Titandioxid P25, Degussa, Ridgefield, NJ; 85 vol % anatase and 15 vol % rutile) was used as a titanium source for lead-based perovskites. Freshly precipitated undried coprecipitated hydrous titania-zirconia was used as a source of titanium and zirconium for Pb(Zr,Ti)-O₃. It was prepared via an alkoxide method modified according to Lencka et al.⁶ in which a solution of titanium tetraisopropoxide 97 vol % in 2-propanol and zirconium tetra-n-propoxide 70 vol % in 2-propanol (Alfa Aesar) was quantitatively hydrolyzed and polymerized to form the hydrous oxide. The oxide content in the hydrous oxide was determined from loss on ignition measurements by heating dried samples in a thermogravimetric analyzer in flowing nitrogen at a rate of 10 °C/min to a temperature of 1000 °C (Perkin-Elmer TGA7, Norwalk, CT).

The reagents were stirred briefly for <1 min in an open 110-mL stainless steel Teflon-lined autoclave (Parr Instruments, Moline, IL) using doubly deionized, filtered (0.22- μ m filter) water (18 Ω·cm, Millipore Corp., Bedford, MA) and a volume

fill of 70%. For the synthesis of PbTiO_3 , the concentration of lead acetate trihydrate was 0.1 M, the molar Pb/Ti and Pb/EDTA ratios were either 1 or 2. For the synthesis of $\text{PbZr}_{0.52}\text{Ti}_{0.48}\text{O}_3$, the concentration of lead acetate trihydrate was 0.1 M, the molar Zr/Ti ratio was 52/48, the molar $\text{Pb}/(\text{Zr} + \text{Ti})$ and Pb/EDTA ratios were 2 and 1, respectively. KOH concentrations were chosen on the basis of thermodynamic calculations. The order of reagent addition was water, lead acetate, EDTA, titania (or hydrous titania-zirconia), and KOH.

Autoclaves were heated (Fisher Scientific, Isotemp Oven, model 655G, ± 3 °C accuracy) at various temperatures ranging from 30 to 200 °C for 72 h. Unstirred reactions were conducted at autogenous pressure. The reaction temperature was limited to 200 °C, because EDTA begins to decompose above this temperature.^{26,27} Experiments were performed at temperature intervals of approximately 20 °C. In selected cases where phase-pure perovskite did not form but was expected, experiments were repeated to confirm the measurement. The reaction products were then cooled to room temperature, vacuum filtered through 0.22-μm Teflon-coated filter paper (Millipore Corp.), and rinsed in 20 vol % ammoniated water to prevent dissolution of the perovskite. The powder was air-dried under ambient conditions overnight. Samples prepared with amorphous titania-zirconia gel were further heat-treated at 600 °C for 3.5 h to crystallize amorphous phases that might not be detected in the room-temperature hydrothermal reaction product.

Product Characterization. The precipitated powders were characterized by using X-ray diffraction (XRD, model D-500, Siemens Analytical X-ray Instruments, Madison, WI), transmission electron microscopy (TEM, model EM-002B, ABT, Tokyo, Japan; model 100CX, JEOL, Tokyo, Japan) accompanied with energy-dispersive spectroscopy (EDS) and field emission scanning electron microscopy (FESEM, model Gemini DSM-982, Leo Zeiss, Germany). The supernatant (liquid after separation from the solid) was quantitatively analyzed for Pb ions by atomic absorption spectroscopy (AAS, model 6500, Perkin Elmer, Norwalk, CT).

XRD was performed on a Siemens D-500 diffractometer using Ni-filtered $\text{CuK}\alpha$ radiation at 40 keV and 30 mA, with divergent slit of 1°, and receiving slit of 0.15°, and a degree step of 0.05° for 2θ and count times of 1–10 s per step. A small representative sample of the product was prepared on plastic amorphous microscope covers and set on an amorphous plastic substrate. Silicon was used as an internal standard when necessary for phase identification. The chemical identity of the products was determined by comparing the experimental X-ray patterns to standards compiled by the Joint Committee on Powder Diffraction and Standards (JCPDS).²⁸

Bright-field TEM was performed on the JEOL 100CX at 100 keV and on the ABT EM-002B at 200 keV. To prepare a TEM specimen, a representative sample of hydrothermal powder was suspended in ethyl alcohol. Carbon-coated copper grids were subsequently dipped into the suspension and dried in vacuo for 24 h. Selected area electron diffraction was used to confirm powder crystallinity. Semiquantitative EDS was used to check for Pb, Zr, and Ti to confirm the completion of the reaction and purity of the powder. EDS was accomplished over an energy range 0–40 keV with a beam size of 8.8 nm and a residence time of 200 s.

FESEM was performed at 5 keV. Powders were deposited and adhered to an aluminum stub coated with carbon adhesive and subsequently coated with carbon to minimize charging.

Solutions used for AAS were prepared by diluting the filtered supernatant in an appropriate acidic (acetic acid and nitric acid) matrix to prevent ions from precipitating. Three standards from a 1000 Pb ppm stock solution (SPEX, Edison, NJ) were prepared by dilution in a matrix of appropriate proportions of KOH, EDTA, and acids. AAS was performed

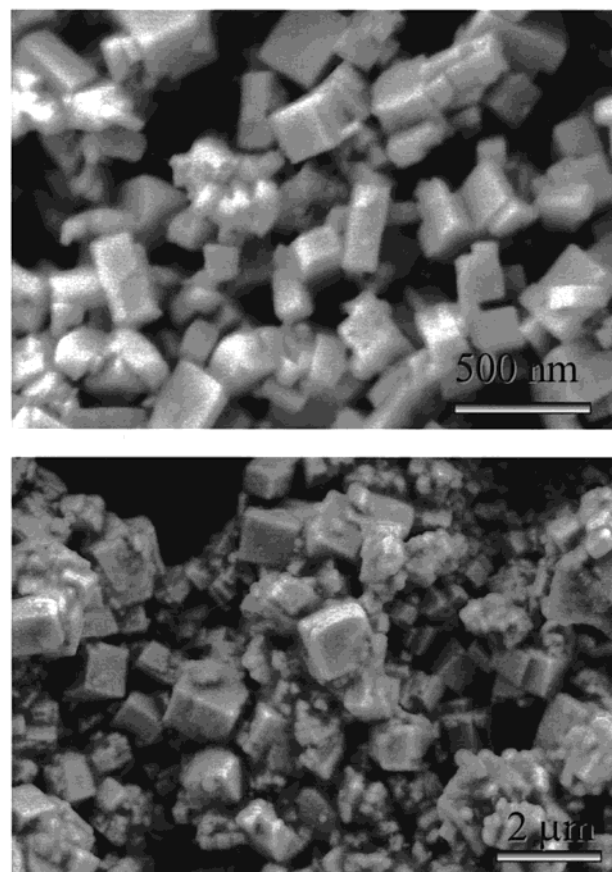


Figure 6. FESEM photomicrographs of (a) phase-pure PbTiO_3 prepared with 0.1 M PbAc_2 , $\text{Pb}/\text{Ti} = 2$, $\text{Pb}/\text{EDTA} = 1$, KOH = 1.15 M, and 0.2 M TiO_2 at 90 °C, 72 h and (b) phase-pure $\text{PbZr}_{0.52}\text{Ti}_{0.48}\text{O}_3$ prepared with 0.1 M PbAc_2 , $\text{Pb}/\text{Ti} = 2$, $\text{Pb}/\text{EDTA} = 1$, KOH = 2.5 M, and 0.05 M $\text{Zr}_{0.52}\text{Ti}_{0.48}\text{O}(\text{OH})_2$ at 147 °C, 72 h.

with an air–acetylene mixture to fuel the flame. Measurements were performed at 217.3 nm for Pb detection.

Results and Discussion

The experimental conditions used for PbTiO_3 (PT) and $\text{Pb}(\text{Zr}_{0.52}\text{Ti}_{0.48})\text{O}_3$ (PZT) are shown in Table 2 and Figures 4 and 5. Yellow powders with platelet and cuboid morphologies were typically found for PT and PZT powders, respectively (Figure 6). The particle size of PT spanned 0.1–0.5 μm, whereas the PZT had a broader particle size distribution of about 0.1–1.5 μm.

Figures 4 and 5 and Table 2 show that numerous reaction conditions using EDTA successfully synthesized phase-pure PT and PZT. No secondary unary lead-based phases were detected in these samples as determined by XRD, regardless of the Pb/Ti stoichiometry used. In general, X-ray line broadening was observed with hydrothermal products, which increased with decreasing reaction temperature, which suggested the presence of amorphous phases. However, selected area electron diffraction of hydrothermal reaction products revealed that both PT and PZT products were crystalline. Furthermore, heat treatment of hydrothermal powders at 600 °C for 3.5 h failed to reveal any secondary phases. Our phase analysis for both PT and PZT systems was well supported by AAS and TEM/EDS data. For PT or PZT reactions using $\text{Pb}/(\text{Ti} + \text{Zr})$ molar ratios of 1.0, AAS determined that supernatant solu-

(27) Wang, H. W.; Hall, D. A.; Sale, F. R. *J. Therm. Anal.* **1994**, 42, 823.

(28) McLane, W. F., Ed. *Powder Diffraction File: Inorganic Phases*; JCPDS International Centre for Diffraction Data: Swarthmore, PA, 1989.

tions from hydrothermal crystallization reactions yielding X-ray phase-pure powders contained less than 1% of input lead species. For PT or PZT reactions using Pb/(Ti + (Zr)) molar ratios of 2.0, 50% of the input lead was found in the supernatant. These results indicate that reactions went at least to 99% completion. TEM/EDS studies on both PT and PZT particles detected the lead, titanium, and zirconium cations expected for these respective powders.

Past work has shown that when the Pb/Ti ratio is greater than 1.0 without EDTA additions, significant proportions of unary lead-based phases form with the exception of conditions that span very narrow pH ranges.^{2,6} This work demonstrates that EDTA is successful in suppressing the formation of lead-bearing secondary phases, as predicted by thermodynamic computations. Based on calculations discussed earlier for solutions containing uncomplexed lead (e.g., Pb/EDTA ratios of 2.0), it is possible that free lead ions could be converted to unary lead phases at room temperature during precursor preparation. However, in these systems, there is a suitable reservoir of Pb-EDTA complexes that can supply the hydrothermal reaction for perovskite formation. As this takes place, the dissociation of Pb-EDTA frees up EDTA to react either with dissolved lead ions or with traces of solid phases such as PbO.

Table 2 shows that the addition of EDTA also reduced the minimum reaction temperature for forming phase-pure perovskite during a three-day period. The minimum reaction temperature for phase-pure PT formation was reduced from 140 to 70 °C. For PZT, the minimum reaction temperature was reduced from 150 to 125 °C. This reduction in temperature may be attributed to the ability of EDTA to provide soluble forms of lead. It may not be critical that all insoluble lead is eliminated at the onset of the reaction but instead that an ample supply of soluble species is always available to diffuse rapidly to the site of PT or PZT crystallization. Without EDTA, dissolution of phases such as PbO may limit the rate of the crystallization process by starving the reaction of soluble lead unless sufficiently high temperatures are used. In cases where unary phases such as PbO might precipitate during precursor preparation (i.e., Pb/Ti = 2.0 and Pb/EDTA = 2.0), EDTA may serve to accelerate the dissolution rate of unary lead phases relative to what is observed without EDTA, ensuring a steady-state supply of lead ions is available.

All hydrothermal systems exhibited a threshold temperature beyond which the thermodynamic model apparently was applicable. The threshold temperature is shown by vertical lines in Figures 4 and 5, which represent an average of the temperatures in a 99% yield region between which a reaction has gone to completion (i.e., minimum reaction temperature) and the temperature where the reaction is incomplete. Below this temperature, sluggish kinetics produced a variety of undesirable phase assemblages. This threshold temperature varied with precursor system. Increasing the Pb/EDTA or Pb/Ti ratios from 1 to 2 served to reduce the threshold temperature from 110 to 80 °C. Each variable seems to be equally important in lowering the threshold temperature. Increasing both ratios at the same time reduced this threshold temperature to as low as 60 °C.

Examining conditions above the threshold temperature and minimum KOH concentrations required for formation of single-phase PT, the computational model apparently successfully predicts PT formation for most conditions. For PZT, there seems to be less agreement, particularly at the lower KOH concentrations. Although the data points suggest that the movement of phase boundaries as a function of Pb/EDTA and Pb/Ti ratios seems correct, additional experimental data points are required to precisely substantiate the model.

Above the threshold temperature, the thermodynamic model predicts the experimental data points for phase fields for unreacted and partially reacted systems poorly. For example, Figure 4f displays reactions at 200 °C and 0.30 M KOH where PbTiO₃ and TiO₂ should coexist. However, under these reaction conditions only TiO₂ was formed. Important factors include experimental errors attributed to XRD methodologies, and hydrothermal experimentation, and the limitations of the thermodynamic model. XRD methods are constrained by high detection limits (>5 vol %) and its inability to detect amorphous phases.²⁹ Hydrothermal experimentation error includes lack of stirring during the reaction and inaccurate assay and tarring. Errors related to the thermodynamic model could include the many limitations of the database used for the calculations discussed earlier.

The importance of using thermodynamics in guiding experiments can be seen through examples of experiments that were not guided by a model. Kim and Matijevic¹⁸ used EDTA to attempt PbTiO₃ synthesis. However, instead, amorphous TiO₂ resulted with use of the following reaction conditions: 0.1 M Pb(NO₃)₂, 0.55 M H₂O₂, 0.4 M HCl, 2.0 M NH₄OH, 0.1 M Na₂H₂-EDTA, and 0.1 M titanium tetra-isopropoxide in H₂O at temperatures ranging from 45 to 100 °C. Thermodynamic modeling was used to determine whether it was possible that their results were governed by equilibrium chemistry. Because thermodynamic properties were not available for titanium tetra-isopropoxide and Na₂H₂-EDTA, 0.1 M TiO₂ and 0.1 M NaH₃EDTA were substituted to facilitate calculations. The substitution of TiO₂ for titanium tetra-isopropoxide was justified because it hydrolyzes and polymerizes to precipitate hydrous titania at room temperature. To account for the extra hydronium ion and sodium ion deficiency introduced by using NaH₃EDTA instead of Na₂H₂EDTA, 0.1 M NaOH was also added. All other reaction conditions were used in the calculation as reported by Kim and Matijevic. The computations produced yield diagrams with incipient precipitation and 99% yield boundaries that shifted minimally by 0.5 pH units. For the specific reaction conditions used by Kim and Matijevic, our calculations indicate that TiO₂ is the stable phase. Because the yield diagrams are similar, we plotted the simulated results of Kim and Matijevic for the temperature and corresponding equilibrium pH on Figure 4a. Our simulations show that their experiments are more than 2 pH units from the appropriate conditions required for phase-pure PT formation.

Preliminary calculations were performed for another precursor system investigated by Kim and Matijevic,

(29) Wachtman, J. B. *Characterization of Materials*; Butterworth-Heinemann, Woburn, MA, 1993; p 299.

where nitrilotriacetic acid was used instead of EDTA. Under these conditions, an amorphous precipitate formed that was calcined to form phase-pure PbTiO_3 . All experimental reaction conditions identified by Kim and Matijevic to form phase-pure PbTiO_3 in this manner were predicted to form PbTiO_3 by the thermodynamic model. This preliminary calculation suggests that our thermodynamic model is suitable for engineering the synthesis of lead-based perovskites from other chelation-based synthesis approaches besides EDTA.

Conclusions

Thermodynamic modeling identified the reaction conditions suitable for synthesis of phase-pure PbTiO_3 and

$\text{PbZr}_{0.52}\text{Ti}_{0.48}\text{O}_3$ using EDTA as the complexing agent for lead species. Computations were useful in finding low-temperature reaction conditions that formed phase-pure powders. EDTA was found to reduce the reaction temperature by as much as 70 °C. The minimum reaction temperature was 70 °C for PbTiO_3 and 125 °C for $\text{Pb}(\text{Zr},\text{Ti})\text{O}_3$. Experiments appeared to validate the yield diagrams constructed from the calculations.

Acknowledgment. We gratefully acknowledge the support of the Office of Naval Research (ONR).

CM000395L